



HAL
open science

Characterizing cardiac phenotype in Friedreich's ataxia: The CARFA study

Lise Legrand, Jonathan Weinsaft, Françoise Pousset, Claire Ewencyk,
Perrine Charles, Stéphane Hatem, Anna Heinzmann, Marie Biet, Alexandra
Durr, Alban Redheuil

► To cite this version:

Lise Legrand, Jonathan Weinsaft, Françoise Pousset, Claire Ewencyk, Perrine Charles, et al.. Characterizing cardiac phenotype in Friedreich's ataxia: The CARFA study. Archives of cardiovascular diseases, 2022, 115 (1), pp.17-28. 10.1016/j.acvd.2021.10.010 . hal-03984825

HAL Id: hal-03984825

<https://hal.science/hal-03984825>

Submitted on 22 Jul 2024

HAL is a multi-disciplinary open access archive for the deposit and dissemination of scientific research documents, whether they are published or not. The documents may come from teaching and research institutions in France or abroad, or from public or private research centers.

L'archive ouverte pluridisciplinaire **HAL**, est destinée au dépôt et à la diffusion de documents scientifiques de niveau recherche, publiés ou non, émanant des établissements d'enseignement et de recherche français ou étrangers, des laboratoires publics ou privés.



Distributed under a Creative Commons Attribution - NonCommercial 4.0 International License

Characterizing cardiac phenotype in Friedreich's ataxia: The CARFA study

Abbreviated title: Characterizing cardiac phenotype in Friedreich's ataxia

Tweet:

Structural and functional variables are necessary to characterize Friedreich Ataxia cardiac phenotype and to evaluate FA cardiac therapeutic targets. No change was observed in cardiac variables at 1 year whereas the neurological severity score increased modestly.

Lise Legrand^{a,b}, Jonathan W. Weinsaft^c, Françoise Pousset^{a,b}, Claire Ewencyk^d, Perrine Charles^d, Stéphane Hatem^{a,b,e}, Anna Heinzmann^d, Marie Biet^d, Alexandra Durr^{d,*}, Alban Redheuil^{b,e,*}

^a *Cardiology Department, Pitié-Salpêtrière Hospital (AP-HP), Sorbonne Université, 75013 Paris, France*

^b *ICAN Institute of Cardiometabolism and Nutrition, 75013 Paris, France*

^c *Weill Cornell Medicine, New York, NY 10021, USA*

^d *Paris Brain Institute (ICM), INSERM, CNRS, Pitié-Salpêtrière Hospital (AP-HP), Sorbonne Université, 75646 Paris, France*

^e *ICT Cardiothoracic Imaging Unit, Pitié-Salpêtrière Hospital (AP-HP) ; Laboratoire d'Imagerie Biomédicale, Sorbonne Université, INSERM, CNRS, 75013 Paris, France*

* Corresponding author at: ICT Cardiothoracic Imaging Unit, Institut de Cardiologie, Hôpital Pitié-Salpêtrière, 47–83 Boulevard de l'Hôpital, 75013 Paris, France.

E-mail address: alban.redheuil@aphp.fr (A. Redheuil).

* Corresponding author at: Institut du Cerveau-Paris Brain Institute (ICM), Pitié-Salpêtrière Hospital, Sorbonne Université, CS21414, 75646 Paris CEDEX 13, France.

E-mail address: alexandra.durr@icm-institute.org (A. Durr).

Dr Lise Legrand and Dr Jonathan W. Weinsaft contributed equally to this work.

Summary

Background. – Friedreich's ataxia is an autosomal recessive mitochondrial disease caused by a triplet repeat expansion in the frataxin gene (*FXN*), exhibiting cerebellar sensory ataxia, diabetes and cardiomyopathy. Cardiac complications are the major cause of early death.

Aims. – To characterize the cardiac phenotype associated with Friedreich's ataxia, and to assess the evolution of the associated cardiopathy over 1 year.

Methods. – This observational single-centre open label study consisted of two groups: 20 subjects with Friedreich's ataxia and 20 healthy controls studied over two visits over 1 year. All subjects had transthoracic echocardiography, cardiac magnetic resonance imaging, cardiopulmonary exercise testing, quantification of serum cardiac biomarkers and neurological assessment.

Results. – Patients with Friedreich's ataxia had left ventricular hypertrophy, with significantly smaller left ventricular diastolic diameters and volumes and increased wall thicknesses. Cardiac magnetic resonance imaging demonstrated significant concentric left ventricular remodelling, according to the mass/volume ratio, and focal myocardial fibrosis in 50% of patients with Friedreich's ataxia.

Cardiopulmonary exercise testing showed alteration of left ventricular diastolic filling in patients with Friedreich's ataxia, with an elevated VE/VCO₂ slope (ventilatory flow/exhaled volume of carbon dioxide). High-sensitivity troponin T plasma concentrations were higher in subjects with Friedreich's ataxia. None of the previous variables changed at 1 year. Neurological assessments remained stable for both groups, except for the nine-hole pegboard test, which was altered over 1 year.

Conclusions. – The multivariable characterization of the cardiac phenotype of patients with Friedreich's ataxia was significantly different from controls at baseline. Over 1 year there were no clinically significant changes in patients with Friedreich's ataxia compared with healthy controls, whereas the neurological severity score increased modestly.

Résumé

Contexte. – L'ataxie de Friedreich (AF) est une maladie mitochondriale autosomique récessive liée à une répétition anormale de nucléotides sur le gène de la frataxine. Elle associe une atteinte cérébelleuse, un diabète et une cardiomyopathie (principale cause de décès).

Buts. – Cette étude a pour but de caractériser le phénotype cardiologique de l'AF et son évolution à un an.

Méthodes. – 20 patients atteints d'AF et 20 sujets sains ont été inclus avec 2 visites espacées d'un an. Tous ont eu une échocardiographie transthoracique, une imagerie cardiaque par résonance magnétique (IRM), un test à l'effort avec mesure de la VO₂ max, un dosage de biomarqueurs cardiaques sériques et une évaluation neurologique.

Résultats. – Les patients AF avaient par rapport aux sujets sains une hypertrophie ventriculaire gauche (VG) avec des diamètres et des volumes diastoliques significativement inférieurs, des parois ventriculaires gauches plus épaisses, un remodelage concentrique avec un rapport masse/volume augmenté et une fibrose focale en IRM pour 50 % d'entre eux. Les concentrations plasmatiques de Hs-troponine étaient plus élevées et la VO₂ max a montré une altération du remplissage diastolique VG avec une augmentation de la pente VE/VCO₂ (débit ventilatoire/production de CO₂) chez ces patients. Seul le « nine-hole pegboard test », sur le plan neurologique, a augmenté à un an.

Conclusions. – A l'inclusion, l'évaluation cardiologique multiparamétrique des patients atteints d'AF était significativement différente de celle des sujets sains. A un an, il n'y avait pas d'évolution significative de ces paramètres alors qu'il existait une discrète augmentation de la sévérité neurologique des patients AF.

KEYWORDS

Friedreich's ataxia;

MRI;

Echocardiography;

Cardiopulmonary exercise testing;

Hypertrophic cardiopathy

MOTS CLÉS

Ataxie de Friedreich ;

Imagerie par résonance magnétique ;

Échocardiographie ;

Test d'effort cardiorespiratoire ;

Cardiopathie hypertrophique

Abbreviations: CCFS, composite cerebellar functional severity; CMRI, cardiac magnetic resonance imaging; CPET, cardiopulmonary exercise testing; FA, Friedreich's ataxia; GAA, guanine-adenine-adenine trinucleotide; hs-TnT: high-sensitivity troponin T; LGE, late gadolinium enhancement; LV, left ventricle/ventricular; LVEF, left ventricular ejection fraction; NT-proBNP, N-terminal-prohormone of B-type natriuretic peptide; SARA, Scale for the Assessment and Rating of Ataxia; TTE, transthoracic echocardiography; VE/VCO₂, ventilatory flow/exhaled volume of carbon dioxide; VO₂, oxygen uptake.

Background

Friedreich's ataxia (FA) is a rare (3–4 cases per 100,000 individuals) but devastating neuromuscular disorder caused by a guanine-adenine-adenine trinucleotide (GAA) repeat expansion in the frataxin (*FXN*) gene [1] that results in reduced expression of frataxin, a mitochondrial protein involved in the biosynthesis of iron-sulphur clusters [2]. FA is characterized by impaired coordination as a result of cerebellar and sensory deficits, the clinical progression of which is impacted by the GAA repeat expansion – the larger the repeat, the lower the frataxin levels and the more severe the disease course.

FA-induced alterations in mitochondrial physiology can affect the heart. Left ventricular (LV) concentric remodelling has been well described in patients with FA, paralleled by decreased chamber volume [3]. Whereas systolic function is often preserved in mild or early-stage disease, impaired contractility can develop progressively. Paralleling altered LV geometry and function, heart failure and arrhythmias have been reported to be common. Cardiac events have been deemed the primary cause of mortality in over half (~60%) of patients with FA – death typically occurs in those aged < 40 years [4, 5].

Despite poor long-term prognosis, the natural history of FA-associated cardiomyopathy varies, and is poorly understood, as evidenced by heterogeneity in disease severity and time course. One reason for the limited understanding of determinants of outcome in FA may stem from the approach used to assess the heart. Transthoracic echocardiography (TTE) has been widely used as a screening tool in patients with FA [6, 7], but this modality relies on geometric assumptions that can be limited in discerning subtle changes in LV remodelling. Cardiac magnetic resonance imaging (CMRI) provides a volumetric reference standard for LV geometry and function that can also assess myocardial tissue properties, including focal and diffuse fibrosis, as discerned by late gadolinium enhancement (LGE) and parametric T1 mapping, respectively [8-10]. Whereas previous CMRI studies identified LV hypertrophy and fibrosis in patients with FA [3, 11-13], it is uncertain whether such alterations in myocardial remodelling and tissue properties are stable over time, and whether these imaging findings impact clinical performance status. Given that the potential for reversal of FA cardiomyopathy has expanded in the context of the preclinical success of gene therapy [14], further research to test imaging surveillance strategies is of growing importance to inform current patient care and future therapeutic trials.

This study encompassed a well-characterized cohort of patients with FA and matched normative controls. Imaging was performed using a standardized multivariable protocol, entailing CMRI and TTE, which was acquired together with clinical, functional (cardiopulmonary exercise testing [CPET]), serum biomarker and genetic profiling. Study goals were to test: (1) TTE and CMRI manifestations of FA-associated LV structural and contractile remodelling; (2) the temporal evolution of cardiovascular imaging indices during prospective follow-up (1 year); and (3) the feasibility, reproducibility and evolution over 1 year of CPET to assess performance status in FA cardiopathy.

Methods

Study population

The study cohort was comprised of adult patients with FA (aged ≥ 18 years) and age/sex-matched normative controls ($n = 20$ per group), each of whom underwent baseline and follow-up assessments over a prespecified 1-year interval.

Patients with FA who met the following criteria were eligible for study participation: diagnostic confirmation based on phenotype and genotype, with associated cardiac involvement based on electrocardiogram or TTE. To avoid confounding by conditions known to confer a high risk of myocardial fibrosis, subjects with FA with known epicardial coronary artery disease or cardiovascular risk equivalents (diabetes mellitus) were excluded. Additional exclusion criteria included contraindication to CMRI (e.g. claustrophobia, non-compatible pacemaker/defibrillator) or gadolinium (known hypersensitivity, glomerular filtration rate < 30 mL/min/1.73 m²), or neurological debility deemed unsafe for exercise testing (CPET).

Normative controls were selected for inclusion based on age/sex matching to patients with FA. Controls were without clinically reported cardiovascular disease or cardiopulmonary symptoms, based on a standardized questionnaire assessment.

All study participants provided written informed consent at the time of enrolment. This study was approved by the relevant ethics and regulatory institutions (CPP Ile de France III N°3327, ANSM N°151261B-21); study details are described further in publicly available databases (ClinicalTrials.gov Identifier: NCT02840669; EUDRACT #: 2015-A01354-45).

Protocol components

TTE

TTE was performed on a VIVID 9 system (GE Healthcare, Chicago, IL, USA) in Pitié-Salpêtrière Hospital; the same expert cardiologist (F. P.) performed all TTE examinations using a standardized protocol. Standard techniques were used to obtain M-mode, two-dimensional and Doppler measurements, in accordance with the recommendations of the American Society of Echocardiography. An independent core laboratory reviewed all examinations, blinded to clinical and genetic data (L. L., Pitié-Salpêtrière Hospital) [15].

Each measure was the mean of three measurements. LV end-diastolic diameter, LV end-systolic diameter, septal wall thickness and posterior wall thickness were measured using standard M-mode from a parasternal long-axis view. LV ejection fraction (LVEF) was calculated using the biplane Simpson method based on two- and four-chamber views. Peak E and A waves were measured by vascular Doppler on the mitral valve. Tissue Doppler imaging was performed on the lateral wall of the left ventricle (Ea). Global longitudinal strain was also calculated according to speckle tracking performed in the apical four-, two- and three-chamber views. By definition, longitudinal strain was a negative number, but the absolute value of longitudinal strain was used in the study.

CMRI

CMRI was performed on a 1.5 Tesla scanner (Aera SOMATOM; Siemens Healthineers, Erlangen, Germany). Following data acquisition and flow analyses at Sorbonne University/Pitié-Salpêtrière Hospital, overseen by an experienced study investigator (A. R.), datasets were transferred to an external CMRI core laboratory (Weill Cornell Medicine, New York, NY, USA) for independent analyses of cardiac remodelling and function. CMRI analyses by the core laboratory have previously been shown to yield high reproducibility for LV geometry [16], function [16, 17] and fibrosis [18] indices, including validation using ex vivo chamber volumes [19] and necropsy-verified LV mass [20] as references.

Cardiac chamber volumes, myocardial mass and function were measured on cine CMRI (steady-state free precession), which included LV long-axis (two, three and four chamber) as well as contiguous short-axis datasets acquired from the atrioventricular (tricuspid and mitral valve) annuli through the LV and right ventricular apices: endocardial border planimetry was performed at end-diastole and end-systole to calculate LV and right ventricular stroke volumes and ejection fraction;

epicardial border planimetry was performed at end-diastole to calculate LV mass (which included papillary muscles and trabeculae). Additional CMRI-measured remodelling variables included end-systolic atrial chamber area, as well as ventricular diameters and regional wall thickness. Flow was analysed using phase-contrast through-plane velocity-encoded gradient echo sequences acquired perpendicular to the ascending tubular aorta and mitral leaflet tips; maximal velocity encoding was set to avoid signal aliasing (typically 1.7 m/s). A validated method based on a robust flow component delineation and automated quantitative variable extraction was used to generate aortic and transmitral flow indices and myocardial velocity data [21].

CMRI tissue characterization included assessment of both focal and diffuse LV fibrosis; diffuse myocardial fibrosis was assessed on parametric T1 mapping, which was acquired pre- and (10 minutes) postcontrast using a modified look-locker inversion recovery (MOLLI) sequence acquired in three equidistant landmarks (base, mid, apex) throughout the left ventricle (LV). T1 data were used to calculate extracellular volume fraction concordant with established guidelines [22]. Focal myocardial fibrosis was assessed on LGE CMRI, which was acquired using an inversion recovery pulse sequence, 10–30 minutes after gadolinium infusion (0.2 mmol/kg) in orientations matched to cine CMRI. Focal fibrosis was localized using a standard 17-segment model; extent (% LV myocardium) was measured based on regional transmural extent of enhancement (based on the midpoint of each affected segment), concordant with established methods [23].

CPET

CPET was performed on an arm bicycle ergometer. The exercise protocol to test the functional capacity of patients with FA consisted of increasing the workload by 5 watts per minute to enable patients with FA to sustain the test. After a warm-up period, subjects were instructed to pedal at 50–60 rpm and to keep pedalling at a constant rate during the test. The test ended on exhaustion. Heart rate and electrocardiogram were recorded during the exercise test. To lower the learning curve, CPET was performed twice during the first visit (on day 1 and day 2). Work VO_{2max} and anaerobic threshold (load value in watts) were recorded to assess physical capacity. Peak oxygen uptake (VO_{2max} in mL/min/kg), VO_2 anaerobic threshold and aerobic VE/ VCO_2 slope (ventilatory flow/exhaled volume of carbon dioxide) were used to reflect cardiopulmonary function.

Plasma concentration of cardiac biomarkers

The blood cardiac biomarkers that were tested included: high-sensitivity troponin T (hs-TnT), a marker of myocardial injury; N-terminal-prohormone of B-type natriuretic peptide (NT-proBNP), a marker of cardiac elevated filling pressure related to heart failure; and galectin 3, a beta-galactoside-binding lectin, currently proposed as a biomarker of heart failure, which reflects cardiac remodelling and fibrosis [24].

Neurological evaluation

Cerebellar ataxia was evaluated using two scales: the Scale for the Assessment and Rating of Ataxia (SARA), which has eight items and a total score of 0 (no ataxia) to 40 (most severe ataxia), and assesses gait, stance, sitting, speech disturbance, finger chase, nose-finger test, fast alternating hand movements and heel-shin slide; and the Composite Cerebellar Functional Severity (CCFS) score, which is a quantitative performance-based scale (freely available at <https://institutducerveau-icm.org/en/tutorial-for-making-ccfs-board/>) that is used to measure the severity of cerebellar signs in the upper limbs, independent of age [25], and has been validated in adults and children [26]. The CCFS score includes two functional tests for the dominant hand: the nine-hole pegboard test (time required to place dowels in nine holes); and the click test (time required to perform 10 cycles). The two tests are adjusted for age by calculating Z-scores, which are then added together [27]

Time course

The study was conducted over two visits from 2016 to 2017. Subject participation was 12 months (\pm 1 month), and the entire study lasted approximately 23 months, including screening, enrolment (over 40 weeks) and study participation. Visit 1 lasted for 2 days: day 1 involved blood test assessment, cardiological evaluation, cardiac testing (including electrocardiogram, Holter electrocardiogram, TTE and CMRI and the first CPET) and a neurological evaluation (SARA score, CCFS and fatigue severity assessment) [27, 28]; on day 2, patients performed another CPET test to assess reproducibility. Visit 2 took place 1 year later, and involved the same examinations as on day 1 of visit 1 (except for the Holter electrocardiogram), performed over 1 day.

Statistical methods

Control subjects were used to establish a normal range and to provide control information for all study assessments. Simple statistical analysis was used to evaluate the variability of the tested variables across and within individuals; non-parametric tests with corrections were performed. Descriptive summaries included means \pm standard deviations and standard errors (ranges) for continuous variables, and counts and percentages for categorical variables (percentages are based on the number of subjects with available data). We compared the performance of LV morphological indices to predict cardiac remodelling associated with FA using receiver operating characteristic analysis. All *P* values are two-sided, and were considered significant at the two-sided 0.05 level of significance, unless otherwise specified. The sample size could not be the focus, as this was an observational study, not a clinical trial, and because there were multiple and multimodality phenotypes across groups. SAS software, version 9.4 (SAS Institute, Cary, NC, USA) was used for all analyses. Given the nature of this exploratory study, there was no imputation of missing data and no interim analysis. However, all analyses were first performed after visit 1 data were collected and were repeated after visit 2.

Results

We included 20 patients with FA and 20 controls. Baseline population characteristics are described in [Table 1](#). All patients completed the study, except one control subject (for personal reasons); no patient was lost to follow-up, and no major adverse event was recorded.

All patients had genetically confirmed FA. The number of GAA repeats on allele 1 (GAA1) was 544 ± 215 base pairs (bp) and on allele 2 (GAA2) was 759 ± 240 bp. Two patients had point mutations 482+1G>C intron 4 and c.3171>G (p.Leu106) in addition to the GAA expansion on one allele. Mean age at inclusion was 29 ± 7 years. Half of the patients with FA were wheelchair bound, 5% were ambulatory with assistance and 45% were ambulatory. None of the subjects had modifiable cardiovascular risk factors – in particular, no systemic hypertension.

Electrical data: Electrocardiogram and Holter electrocardiogram

Heart rate at baseline was significantly higher in subjects with FA compared with controls (76 ± 12 vs 61 ± 11 beats/min; $P < 0.001$) and was unchanged after 1 year of follow-up. PR interval was significantly shorter in subjects with FA compared with control subjects at visits 1 and 2 (110 ± 1 vs

125 ± 23 ms [$P = 0.03$] and 111 ± 14 vs 129 ± 19 ms [$P = 0.002$], respectively), and was unchanged at 1 year. At visit 1, Holter electrocardiogram results showed that atrial ectopic beats were more frequent in subjects with FA compared with controls (809 ± 2394/24 hours vs 18 ± 46/24 hours; $P = 0.003$).

There were no doublets or sustained ventricular arrhythmias.

TTE

TTE results are presented in [Table 2](#). Patients with FA had significantly smaller LV diastolic diameters and volumes and increased wall thickness. LV mass was significantly higher in subjects with FA than in controls and was unchanged over 1 year. LVEF was normal in the two groups, with no significant change over 1 year. E peak (early ventricular filling velocity) was statistically lower in subjects with FA than in control subjects at both visits, but did not change over 1 year. LV global longitudinal strain was lower in subjects with FA than in control subjects at visit 1 in terms of absolute value (17% vs 19%; $P = 0.002$) and at visit 2 (18% vs 20%; $P < 0.001$). There was no change in global longitudinal strain over 1 year in patients with FA, and the difference found in controls was not clinically relevant. Left atrial dimensions (diameter, volume) were similar in both groups at visits 1 and 2. Nevertheless, we found a significant increase over 1 year in left atrial volume in patients with FA. Tricuspid annular plane systolic excursion (TAPSE) was lower in patients with FA than in controls at visit 1, with no change over 1 year.

CMRI

No CMRI data components were considered uninterpretable, and motion and/or gating artefacts were found in only five (17%) of all participants, making CMRI highly feasible in this potentially challenging setting.

Cardiac morphology and function

LV end-diastolic dimensions (diameter, volume and volume index) were markedly smaller in patients with FA compared with controls at visits 1 and 2. LV end-diastolic diameter was 47 ± 6 mm (FA group) vs 52 ± 3 mm (control group) at visit 1, and 48 ± 5 mm (FA group) vs 53 ± 5 mm (control group) at visit 2. Similar results were seen for LV end-diastolic volume: 144 ± 35 mL (FA group) vs 154 ± 31 mL (control group). LV stroke volume was lower in patients with FA compared with controls at visits 1 and

2, without significant change over one 1 year (*P* value not significant). LVEF remained normal in both groups, and there was no change over 1 year.

CMRI results are summarized in [Table 3](#) and illustrated in [Fig. 1](#). LV thickness was increased in patients with FA compared with controls. Anteroseptal and inferolateral thicknesses were greater in patients with FA than in controls, without significant change over 1 year in either group. The LV mass/volume ratio was also markedly increased in patients with FA compared with controls, without significant change over 1 year. The sensitivity and specificity of the LV mass/volume ratio to identify patients with FA from controls were 95% and 89%, respectively, with an area under the curve of 0.97 (95% confidence interval 0.92–1.00; *P* < 0.001), whereas the sensitivity and specificity of the LV mass index were 70% and 74%, respectively, with an area under the curve of 0.80 (95% confidence interval 0.66–0.93; *P* = 0.002). E peak (early ventricular filling velocity) was lower in subjects with FA than control subjects at both visits, and the difference was not statistically significant over 1 year. Left atrial diameter and area were smaller in patients with FA at visits 1 and 2, and the change was not significant over 1 year.

Concerning right ventricular chamber remodelling, ventricular and atrial dimensions were smaller in patients with FA than in controls, but there were no significant changes over 1 year.

Myocardial tissue characterization

Half of subjects with FA demonstrated myocardial LGE, which was absent in all controls. In all LGE-positive cases, the distribution pattern was typically focal in the lateral wall, intramural or epicardial, in favour of a non-ischaemic process ([Figs. 2 and 3](#)). Overall, LGE extension was modest, representing < 2% of myocardial volume and an average of 1.5 out of 17 American Heart Association segments. Patients with FA with LGE were more hypertrophic, with an increased LV mass index (98 ± 21 vs 79 ± 11 g/m²; *P* = 0.02), and tended to have increased concentric remodelling (mass/volume ratio 1.46 ± 0.29 vs 1.31 ± 0.25 g/mL; *P* > 0.05) compared with patients with FA without LGE. Native and postcontrast myocardial T1 values were slightly lower than in controls at baseline (962 ± 30 vs 989 ± 36 ms [*P* = 0.02] and 376 ± 53 vs 410 ± 46 ms [*P* = 0.04], respectively), but without significant change over 1 year. Extracellular volume was not significantly different between groups at baseline, and values were within the normal range.

CPET

CPET results for visits 1 and 2 are presented in [Table 4](#). There was no difference concerning the reproducibility of CPET results for FA and control subjects at visit 1 (day 1 versus day 2); for all variables the *P* value was > 0.1.

CPET capacity (watts) was lower in subjects with FA compared with control subjects at each visit, and for subjects with FA, CPET capacity decreased slightly over 1 year between the two groups (*P* = 0.03).

VO_{2max} for subjects with FA was lower than for control subjects at visit 1 (*P* < 0.001) and visit 2 (*P* < 0.001); the change over 1 year was not statistically significant. VO₂ anaerobic threshold was also significantly lower for subjects with FA than control subjects (*P* = 0.003) at visit 1. For these two variables, the decrease over 1 year for each group was not statistically significant, nor was the difference between the groups. VE/VCO₂ slope values were significantly higher in subjects with FA than in control subjects at visits 1 and 2; no difference was observed after 1 year.

Circulating biomarkers

The hs-TnT concentration was significantly higher in subjects with FA compared with control subjects at visits 1 and 2 (respectively, 26 ± 28 vs 4 ± 2 ng/L at visit 1 [*P* < 0.001] and 20 ± 16 vs 5 ± 4 ng/L at visit 2 [*P* < 0.001]). The difference between groups over 1 year was not statistically significant (*P* = 0.122). The cut-off value for hs-TnT was 14 ng/L.

Galectin 3 plasma concentrations were significantly higher in patients with FA than in control subjects at visit 1 (12 ± 2 vs 10 ± 2 ng/L; *P* = 0.006), with no significant change over 1 year.

Plasma concentrations of NT-proBNP remained within the normal range at visits 1 and 2 for patients and controls (respectively, 75 ± 200 vs 23 ± 16 ng/L at visit 1 [*P* = 0.9] and 62 ± 135 vs 32 ± 26 ng/L at visit 2 [*P* = 0.6]). The change over 1 year was not clinically relevant (*P* = 0.05).

Neurological assessments

SARA score

The SARA score was higher in patients with FA than in controls at visits 1 and 2 (*P* < 0.001). The mean SARA score was 22 ± 8 in patients with FA at visit 1 and remained stable at visit 2.

CCFS score

The CCFS score was higher in patients with FA than in controls ($P < 0.001$); it increased significantly over 1 year in FA ($P = 0.003$), showing its sensitivity to slow neurological change.

Safety data

A summary of adverse events organized by System Organ Class is presented in [Table A.1](#). Only one adverse event was deemed to be related to study procedures: one patient in the FA group had suspicion of myocardial infarction possibly related to CPET, but this was not confirmed: there was no troponin elevation and no coronary artery disease on the coronary angiogram.

Discussion

The objective of this observational study was to characterize the early phenotype of the cardiomyopathy associated with FA using a multimodal approach, including CPET, TTE, CMRI and serum biological markers, and to assess their evolution over 1 year. The underlying goal was to provide new endpoints for subsequent clinical studies evaluating therapeutic options for FA-related cardiomyopathy.

Historic in vivo data describing the cardiac phenotype in FA have mainly described LV hypertrophy – both electrical by electrocardiogram and in imaging from two-dimensional echocardiography. Existing data suggest a progressive continuum of cardiac involvement, from early electrical anomalies to later occurrence of cardiac hypertrophy and dense fibrosis, ultimately leading to cardiac dysfunction [11]. However, 60% of patients with FA have septal hypertrophy on echocardiography, and only 50% of patients have a CMRI-confirmed increase in LV mass or wall thickening. Early and precise multimodality biomarkers are therefore required to identify early stages of FA-related cardiomyopathy, to ultimately provide targets for emerging therapies.

In the present study, we found – as expected – increased LV wall thickness and increased LV mass in patients with FA, on both echocardiography and CMRI, which served as a reference method for such measurements. Subjects with FA demonstrated lower stroke volume, consistent with LV hypertrophy and concentric remodelling. LVEF remained normal, partly because of small LV volumes in subjects with FA. These data are consistent with the existing literature [3, 7]. Concentric remodelling, measured on CMRI as an increased end-diastolic mass/volume ratio, was found to have

the highest sensitivity and specificity to detect FA-related cardiomyopathy compared with LV mass index, also measured by CMRI. However, we found no clinically significant changes in biventricular and atrial morphological and functional measures at 1 year.

This study showed that CPET was feasible and reproducible, and could be performed safely in subjects with FA [3]. Patients with FA had reduced CPET capacity compared with control subjects at both visits, indicative of reduced cardiopulmonary efficiency and lower exercise tolerance as a result of cardiovascular and/or muscular limitation. The decrease in VO_2 load, with unchanged peak VO_2 over 1 year, was possibly related to deterioration in muscle mass and/or decreased energetic efficiency, and was not indicative of worsening heart function, as both echocardiography and CMRI showed a normal LVEF. The VE/VCO_2 slope, a measure in CPET of the quality of the balance between pulmonary ventilation and perfusion, was significantly increased in subjects with FA compared with controls. In the absence of pulmonary disease, this increase could reflect alterations in LV diastolic filling that could be an early indication of cardiac remodelling, as quantified by CMRI. However, no evolution of the CPET-measured variables was observed over 1 year in patients with FA.

Concerning non-invasive CMRI tissue characterization, we found half of patients with FA to have lateral subepicardial or transmural LGE, indicative of dense replacement fibrosis. LGE has previously been shown to be associated with severe or end-stage forms of FA-related cardiomyopathy [11]. Accordingly, in the present study, individuals with LGE had a higher LV mass index and mass-to-volume ratio than those without LGE. The areas of the myocardium remote to LGE had lower native and postcontrast T1 values compared with matched healthy controls. Decreased postcontrast myocardial T1 has been shown to be related to extracellular matrix expansion and adverse outcomes in several other disease settings [29, 30], even in the absence of elevated native T1 or extracellular volume [30]; this may suggest the presence of interstitial diffuse fibrosis in FA-related cardiomyopathy, even in the absence of dense fibrosis, as depicted by LGE. This finding is also consistent with histological data from Koeppen et al. [31], demonstrating extensive and diffuse endomyocardial fibrosis to be a central finding in FA myocardial pathology samples. However, the variability in postcontrast T1 acquisition and measurement is well known, and must be underlined, as well as the magnitude of differences found, which reflect the relatively small sample size in this rare disease and a potential lack of power, which may also explain the variations found in controls and the absence of differences found in extracellular volume at baseline. Of note, we found native T1 to be lower in patients with FA

compared with controls, whereas this variable is usually described as being increased in fibrotic myocardium [30]. This may be explained in part by diffuse myocardial iron deposits in FA, which have also been described in histology [32]. Myocardial iron overload is known to decrease CMRI T1 relaxation times, and may consequently offset the expected increase in T1 related to fibrosis in this setting. However, this hypothesis remains to be explored. Neither LGE nor T1 mapping-derived indices changed significantly over 1 year.

Plasma concentrations of hs-TnT were elevated in patients with FA. We reported previously that troponin is positively correlated with maximum septal LV wall thickness in echocardiography [33]. Weideman et al. reported that hs-TnT concentrations were raised in subjects with FA with more severe cardiac disease with LGE on CMRI [11]. Elevated hs-TnT concentrations could reliably reflect ongoing subclinical myocyte injury, subsequently leading to fibrosis in FA cardiomyopathy, mainly driven by mitochondrial dysfunction, independent of coronary disease. The precise mechanism of myocyte injury and release of hs-TnT remains unsolved.

The nine-hole pegboard test (part of the CCFS), a sensitive clinical marker for cerebellar involvement in FA, evaluating clinical severity, increased significantly over 1 year in patients with FA ($P < 0.01$). However, as mentioned above, this was not concurrent with significant cardiovascular structural and functional deterioration over the same period.

Study limitations

We proposed a comprehensive evaluation of cardiac phenotype in FA, in a relatively small group of young adult patients, which may induce a lack of statistical power. We observed some statistically significant variations between the two groups, with no clinical significance. Furthermore, studied patients needed to be able to undergo CMRI and CPET, so those with the most advanced disease could not be included. Results cannot be extrapolated directly to patients with diabetes with FA, as such patients were excluded.

Conclusions

Changes in cardiac phenotype were somewhat modest over 1 year of follow-up in patients with FA compared with healthy volunteers, whereas the slowly progressive neurological involvement in FA was picked up by the functional test in the upper limbs (CCFS).

Multimodality imaging, including cardiac echocardiography and CMRI, and functional endpoints such as CPET should be considered for future cardiac therapeutics trials in FA.

Acknowledgements

We are very thankful and deeply indebted to the patients and their families for participating in this study. Many thanks to the Association Française de l'Ataxie de Friedreich (AFAF) for support and for disseminating information about the study, as well as to Richard Pushkin, Mehdi Gasmi, Brahim Belbellaa, Cesare Orlandi, Shraddha Desai and Herve Villemagne from Adverum Biotechnologies. We also thank Adverum Biotechnologies for the funding of this study

Sources of funding

This study was funded by Adverum Biotechnologies.

Disclosure of interest

The authors declare that they have no conflicts of interest concerning this article.

References

- [1] Durr A, Cossee M, Agid Y, et al. Clinical and genetic abnormalities in patients with Friedreich's ataxia. *N Engl J Med* 1996;335:1169-75.
- [2] Puccio H, Koenig M. Recent advances in the molecular pathogenesis of Friedreich ataxia. *Hum Mol Genet* 2000;9:887-92.
- [3] Weidemann F, Rummey C, Bijmens B, et al. The heart in Friedreich ataxia: definition of cardiomyopathy, disease severity, and correlation with neurological symptoms. *Circulation* 2012;125:1626-34.
- [4] Pousset F, Legrand L, Monin ML, et al. A 22-Year Follow-up Study of Long-term Cardiac Outcome and Predictors of Survival in Friedreich Ataxia. *JAMA Neurol* 2015;72:1334-41.
- [5] Tsou AY, Paulsen EK, Lagedrost SJ, et al. Mortality in Friedreich ataxia. *J Neurol Sci* 2011;307:46-9.
- [6] Payne RM, Wagner GR. Cardiomyopathy in Friedreich ataxia: clinical findings and research. *J Child Neurol* 2012;27:1179-86.
- [7] Regner SR, Lagedrost SJ, Plappert T, et al. Analysis of echocardiograms in a large heterogeneous cohort of patients with friedreich ataxia. *Am J Cardiol* 2012;109:401-5.
- [8] Wong TC, Piehler K, Meier CG, et al. Association between extracellular matrix expansion quantified by cardiovascular magnetic resonance and short-term mortality. *Circulation* 2012;126:1206-16.
- [9] Sado DM, Flett AS, Moon JC. Novel imaging techniques for diffuse myocardial fibrosis. *Future Cardiol* 2011;7:643-50.
- [10] Moon JC, Treibel TA, Schelbert EB. T1 mapping for diffuse myocardial fibrosis: a key biomarker in cardiac disease? *J Am Coll Cardiol* 2013;62:1288-9.
- [11] Weidemann F, Liu D, Hu K, et al. The cardiomyopathy in Friedreich's ataxia - New biomarker for staging cardiac involvement. *Int J Cardiol* 2015;194:50-7.
- [12] Raman SV, Phatak K, Hoyle JC, et al. Impaired myocardial perfusion reserve and fibrosis in Friedreich ataxia: a mitochondrial cardiomyopathy with metabolic syndrome. *Eur Heart J* 2011;32:561-7.
- [13] Mehta N, Chacko P, Jin J, et al. Serum versus Imaging Biomarkers in Friedreich Ataxia to Indicate Left Ventricular Remodeling and Outcomes. *Tex Heart Inst J* 2016;43:305-10.

- [14] Perdomini M, Belbellaa B, Monassier L, et al. Prevention and reversal of severe mitochondrial cardiomyopathy by gene therapy in a mouse model of Friedreich's ataxia. *Nat Med* 2014;20:542-7.
- [15] Komajda M, Isnard R, Cohen-Solal A, et al. Effect of ivabradine in patients with heart failure with preserved ejection fraction: the EDIFY randomized placebo-controlled trial. *Eur J Heart Fail* 2017;19:1495-503.
- [16] Janik M, Cham MD, Ross MI, et al. Effects of papillary muscles and trabeculae on left ventricular quantification: increased impact of methodological variability in patients with left ventricular hypertrophy. *J Hypertens* 2008;26:1677-85.
- [17] Kim J, Krichevsky S, Xie L, et al. Incremental Utility of Right Ventricular Dysfunction in Patients With Myeloproliferative Neoplasm-Associated Pulmonary Hypertension. *J Am Soc Echocardiogr* 2019.
- [18] Chinitz JS, Chen D, Goyal P, et al. Mitral apparatus assessment by delayed enhancement CMR: relative impact of infarct distribution on mitral regurgitation. *JACC Cardiovasc Imaging* 2013;6:220-34.
- [19] Codella NC, Weinsaft JW, Cham MD, Janik M, Prince MR, Wang Y. Left ventricle: automated segmentation by using myocardial perfusion threshold reduction and intravoxel computation at MR imaging. *Radiology* 2008;248:1004-12.
- [20] Codella NC, Lee HY, Fieno DS, et al. Improved left ventricular mass quantification with partial voxel interpolation: in vivo and necropsy validation of a novel cardiac MRI segmentation algorithm. *Circ Cardiovasc Imaging* 2012;5:137-46.
- [21] Bollache E, Redheuil A, Clement-Guinaudeau S, et al. Automated left ventricular diastolic function evaluation from phase-contrast cardiovascular magnetic resonance and comparison with Doppler echocardiography. *J Cardiovasc Magn Reson* 2010;12:63.
- [22] Messroghli DR, Moon JC, Ferreira VM, et al. Clinical recommendations for cardiovascular magnetic resonance mapping of T1, T2, T2* and extracellular volume: A consensus statement by the Society for Cardiovascular Magnetic Resonance (SCMR) endorsed by the European Association for Cardiovascular Imaging (EACVI). *J Cardiovasc Magn Reson* 2017;19:75.

- [23] Sievers B, Elliott MD, Hurwitz LM, et al. Rapid detection of myocardial infarction by subsecond, free-breathing delayed contrast-enhancement cardiovascular magnetic resonance. *Circulation* 2007;115:236-44.
- [24] Gehlken C, Suthahar N, Meijers WC, de Boer RA. Galectin-3 in Heart Failure: An Update of the Last 3 Years. *Heart Fail Clin* 2018;14:75-92.
- [25] du Montcel ST, Charles P, Ribai P, et al. Composite cerebellar functional severity score: validation of a quantitative score of cerebellar impairment. *Brain* 2008;131:1352-61.
- [26] Filipovic Pierucci A, Mariotti C, Panzeri M, et al. Quantifiable evaluation of cerebellar signs in children. *Neurology* 2015;84:1225-32.
- [27] Tanguy Melac A, Mariotti C, Filipovic Pierucci A, et al. Friedreich and dominant ataxias: quantitative differences in cerebellar dysfunction measurements. *J Neurol Neurosurg Psychiatry* 2018;89:559-65.
- [28] Marelli C, Figoni J, Charles P, et al. Annual change in Friedreich's ataxia evaluated by the Scale for the Assessment and Rating of Ataxia (SARA) is independent of disease severity. *Mov Disord* 2012;27:135-8.
- [29] Ellims AH, Shaw JA, Stub D, et al. Diffuse myocardial fibrosis evaluated by post-contrast t1 mapping correlates with left ventricular stiffness. *J Am Coll Cardiol* 2014;63:1112-8.
- [30] Ambale-Venkatesh B, Lima JA. Cardiac MRI: a central prognostic tool in myocardial fibrosis. *Nat Rev Cardiol* 2015;12:18-29.
- [31] Koeppen AH, Ramirez RL, Becker AB, et al. The pathogenesis of cardiomyopathy in Friedreich ataxia. *PLoS One* 2015;10:e0116396.
- [32] Koeppen AH. Friedreich's ataxia: pathology, pathogenesis, and molecular genetics. *J Neurol Sci* 2011;303:1-12.
- [33] Legrand L, Maupain C, Monin ML, et al. Significance of NT-proBNP and High-sensitivity Troponin in Friedreich Ataxia. *J Clin Med* 2020;9.

Figure legends

Figure 1. Concentric left ventricular (LV) remodelling in patient with Friedreich's ataxia (FA) versus control in cardiac magnetic resonance imaging; patient with FA: LV ejection fraction 68%, LV mass/volume 1.5; control: LV ejection fraction 68%, LV mass/volume 1.3.

Figure 2. Intramyocardial late gadolinium enhancement (green arrow) of the left ventricular lateral wall in consecutive basal and mid left ventricle T1 weighted inversion recovery short-axis views in a 23-year-old male patient with Friedreich's ataxia.

Figure 3. Cardiac magnetic resonance imaging T1 mapping in Friedreich's ataxia. A. Basal short-axis parametric map of native modified look-locker inversion recovery (MOLLI) sequence T1 relaxation values in a patient with Friedreich's ataxia (A1) and control (A2). B. Basal short-axis parametric map of 15-minute postcontrast MOLLI T1 relaxation values in a patient with Friedreich's ataxia (B1) and control (B2). Gd: gadolinium.

Table 1 Baseline characteristics of patients with Friedreich's ataxia and control subjects.

	FA (<i>n</i> = 20)	Control (<i>n</i> = 20)	<i>P</i>
Women (%)	12 (60)	12 (60)	
Age (years)	29 ± 7	29 ± 6	
Weight (kg)	62 ± 12	70 ± 12	0.04
Height (cm)	170 ± 11	173 ± 8	NS
Body mass index (kg/m ²)	22 ± 3	24 ± 3	NS
Heart rate (beats/min)	76 ± 14	60 ± 11	< 0.001
Systolic blood pressure (mmHg)	109 ± 9	112 ± 7	NS
Diastolic blood pressure (mmHg)	69 ± 9	70 ± 7	NS
Number of GAA repeats			
Allele 1	544 ± 215	NA	
Allele 2	759 ± 240	NA	
FA history: age at first symptoms (years)	15 ± 7	NA	NA
Time living with disease (years)	14 ± 6	NA	NA
SARA score (maximum worst score = 40)	22 ± 8	0.3 ± 0.6	< 0.001
CCFS score (normal range of 0.85 ± 0.05)	1.2 ± 0.142	0.856 ± 0.055	< 0.001

Data are expressed as number (%) or mean ± standard deviation. CCFS: Composite Cerebellar

Functional Severity; FA: Friedreich's ataxia; GAA: guanine-adenine-adenine trinucleotide; NS: not applicable; NS: not significant; SARA: Scale for the Assessment and Rating of Ataxia.

Table 2 Transthoracic echocardiography variables at visit 1 and visit 2.

Variables	Visit 1			Visit 2			<i>P</i> ^a	Change from visit 1 to visit 2	
	FA	Control	<i>P</i> ^b	FA	Control	<i>P</i> ^b		FA <i>P</i> ^c	Control <i>P</i> ^c
	(<i>n</i> = 20)	(<i>n</i> = 20)		(<i>n</i> = 20)	(<i>n</i> = 19)			(<i>n</i> = 20)	(<i>n</i> = 19)
LVEDD (mm)	46 ± 6	50 ± 3	0.02	46 ± 6	51 ± 3	0.006	0.32	0.8	0.03
LVESD (mm)	28 ± 7	31 ± 3	0.09	29 ± 6	31 ± 3	0.08	0.07	0.05	0.95
Diastolic volume biplane (mL)	86 ± 29	104 ± 19	0.02	88 ± 31	101 ± 20	0.09	0.27	0.7	0.3
Systolic volume biplane (mL)	32 ± 16	37 ± 9	0.09	33 ± 15	36 ± 10	0.2	0.4	0.7	0.4
Septal wall thickness (mm)	12 ± 2	9 ± 1	< 0.001	12 ± 2	9 ± 1	< 0.001	0.7	0.8	0.5
Posterior wall thickness (mm)	11 ± 2	8 ± 1	< 0.001	11 ± 2	9 ± 2	0.004	0.3	0.8	0.1
LV mass (g)	187 ± 47	147 ± 30	0.004	175 ± 55	159 ± 41	0.4	0.02	0.1	0.05
LVEF (%)	64 ± 8	65 ± 4	0.7	64 ± 6	65 ± 5	0.6	0.7	0.9	0.5
E (m/s)	0.7 ± 0.1	0.8 ± 0.1	0.005	0.7 ± 0.2	0.9 ± 0.2	0.02	0.7	0.2	0.1
A (m/s)	0.5 ± 0.1	0.5 ± 0.1	0.8	0.5 ± 0.1	0.5 ± 0.1	1	0.7	0.8	0.8
E/A ratio	1.5 ± 0.5	1.6 ± 0.4	0.2	1.5 ± 0.5	1.7 ± 0.5	0.1	0.3	0.3	0.2
E deceleration time (ms)	144 ± 22	164 ± 36	0.09	151 ± 36	154 ± 28	0.6	0.3	0.7	0.4
Ea septal tissue Doppler imaging (cm/s)	10 ± 3	13 ± 4	0.06	12 ± 3	15 ± 3	0.007	0.008	< 0.001	< 0.001
Global longitudinal strain (%)	17 ± 2	19 ± 2	0.002	18 ± 2	20 ± 1	< 0.001	0.5	0.06	0.005

TAPSE (cm/s)	21 ± 4	24 ± 4	0.02	22 ± 4	22 ± 3	0.001	0.5	0.3	0.02
Left atrial volume biplane (mL)	43 ± 7	49 ± 12	0.2	47 ± 11	51 ± 11	0.4	0.2	0.05	0.4

Data are expressed as mean ± standard deviation. A: late ventricular filling velocity; E: early ventricular filling velocity; FA: Friedreich's ataxia; LV: left ventricular; LVEDD: left ventricular end-diastolic diameter; LVEF: left ventricular ejection fraction; LVESD: left ventricular end-systolic diameter; TAPSE: tricuspid annular plane systolic excursion.

^a *P* compares changes between FA versus control during the study

^b *P* value compares FA versus control using the Wilcoxon rank sum test.

^c *P* value assesses significance of the change from visit 1 to visit 2 using the Wilcoxon signed rank test in each group.

Table 3 Cardiac magnetic resonance imaging variables at visit 1 and visit 2.

Variables	Visit 1			Visit 2			<i>P</i> ^a	Change from visit 1 to visit 2	
	FA	Control	<i>P</i> ^b	FA	Control	<i>P</i> ^b		FA <i>P</i> ^c	Control <i>P</i> ^c
	(<i>n</i> = 20)	(<i>n</i> = 20)		(<i>n</i> = 20)	(<i>n</i> = 19)			(<i>n</i> = 20)	(<i>n</i> = 19)
LV wall thickness, anteroseptal (mm)	12 ± 2	8 ± 2	< 0.001	11 ± 2 (<i>n</i> = 19)	8 ± 2 (<i>n</i> = 19)	< 0.001	0.7	0.06	0.07
LV wall thickness, inferolateral (mm)	10 ± 2	7 ± 2	< 0.001	9.6 ± 2 (<i>n</i> = 19)	7 ± 2 (<i>n</i> = 19)	0.003	0.11	0.15	0.4
LV function									
LVEF (%)	62 ± 10	65 ± 5	0.2	62 ± 11	62 ± 5	0.9	0.05	0.6	0.04
LV stroke volume (mL)	68 ± 18	98 ± 22	< 0.001	71 ± 17	99 ± 21	< 0.001	0.114	0.1	0.7
LV cardiac output (L/min)	5.3 ± 1.1	6 ± 1	0.01	5.2 ± 1.2	5.7 ± 0.9	0.09	0.3	0.8	0.1
LV myocardial mass (g)	161 ± 44	137 ± 29	0.04	150 ± 45	128 ± 26	0.1	0.05	< 0.001	< 0.001
LV mass/LVEDV ratio	1.4 ± 0.3	0.9 ± 0.2	< 0.001	1.3 ± 0.2	0.8 ± 0.1	< 0.001	0.30	0.0007	0.003
Left atrial chamber size									
Left atrial diameter (mm)	29 ± 4	33 ± 4	0.01	30 ± 3	33 ± 4	0.006	0.5	0.1	0.5
Left atrial area (cm ²)	17 ± 3	20 ± 4	0.003	16 ± 3	20 ± 4	0.001	0.8	0.8	0.9
Transmitral flow E-wave peak (cm/s)	34 ± 8	43 ± 9	0.006	34 ± 8	42 ± 11	0.01	0.98	0.9	0.6
Transmitral flow A-wave peak (cm/s)	18 ± 5	20 ± 8	0.7	18 ± 5	20 ± 9	0.99	0.9	0.9	0.9
Transmitral flow deceleration time	147 ± 38	156 ± 35	0.4	175 ± 72	166 ± 29	0.8	0.63	0.06	0.2

(ms)									
Net aortic flow (mL)	69 ± 16	92 ± 17	< 0.001	69 ± 15	95 ± 19	< 0.001	0.48	0.6	1.0
Myocardial velocity lateral wall E peak	8 ± 2	12 ± 3	< 0.001	8 ± 2	11 ± 3	0.001	0.84	0.2	0.3
RV chamber size									
RVEDV (mL)	114 ± 33	170 ± 40	< 0.001	117 ± 33	175 ± 38	< 0.001	0.8	0.9	0.5
RVESV (mL)	48 ± 18	75 ± 21	< 0.001	48 ± 17	82 ± 21	< 0.001	0.02	0.5	0.03
Right atrial area (cm ²)	15 ± 4	20 ± 5	< 0.001	15 ± 4	20 ± 4	< 0.001	0.24	0.9	0.06
RV function									
RVEF (%)	58 ± 6	56 ± 5	0.3	59 ± 6	53 ± 4	0.005	0.04	0.5	0.02
RV stroke volume (mL)	66 ± 18	95 ± 22	< 0.001	67 ± 22	93 ± 19	< 0.001	0.15	0.4	0.2
LGE									
Present	10 (50)	0	-	10 (50)	0	-	-	-	-
Extent (% LV myocardium)	17 ± 2.4	0	-	15 ± 2.1	0	-	-	0.47	-
Extent (number of segments)	1.5 ± 2.1	0	-	1.5 ± 2.0	0	-	-	0.67	-
T1 mapping									
Precontrast myocardial T1 (ms)	962 ± 30	989 ± 36	0.02	961 ± 24	978 ± 37	0.2	0.27	1	0.1
Postcontrast myocardial T1 (ms)	376 ± 53	410 ± 46	0.04	369 ± 55	356 ± 55	0.5	0.008	0.7	0.002
Precontrast blood T1 (ms)	1508 ± 81	1544 ± 69	0.08	1531 ± 76	1578 ± 72	0.04	0.224	0.4	0.01
Postcontrast blood T1 (ms)	223 ± 41	237 ± 43	0.3	211 ± 36	196 ± 38	0.2	0.05	0.4	0.002

Haematocrit (%)	43 ± 3	43 ± 4	0.5	43 ± 2	41 ± 3	0.009	0.03	0.98	0.02
Extracellular volume (%)	0.24 ± 0.04	0.23 ± 0.03	0.3	0.23 ± 0.03 (<i>n</i> = 19)	0.24 ± 0.03 (<i>n</i> = 19)	0.6	0.01	0.1	0.07

Data are expressed as mean ± standard deviation or number (%). FA: Friedreich's ataxia; LGE: late gadolinium enhancement; LV: left ventricular; LVEDV: left ventricular end-diastolic volume; LVEF: left ventricular ejection fraction; RV: right ventricular; RVEDV: right ventricular end-diastolic volume; RVEF: right ventricular ejection fraction; RVESV: right ventricular end-systolic volume.

^a *P* compares changes between FA versus control during the study.

^b *P* value compares FA versus control using the Wilcoxon rank sum test.

^c *P* value assesses significance of the change from visit 1 to visit 2 using the Wilcoxon signed rank test.

Table 4 Cardiopulmonary exercise testing variables at visit 1 and visit 2.

Variables	Visit 1			Visit 2			<i>P</i> ^a	Change from visit 1 to visit 2	
	FA (day 2)	Control	<i>P</i> ^b	FA	Control	<i>P</i> ^b		FA <i>P</i> ^c	Control <i>P</i> ^c
	(<i>n</i> = 20)	(<i>n</i> = 20)		(<i>n</i> = 20)	(<i>n</i> = 19)			(<i>n</i> = 20)	(<i>n</i> = 19)
Work VO _{2max} (watts)	58 ± 22 (<i>n</i> = 19)	88 ± 39 (<i>n</i> = 19)	< 0.001	44 ± 19	88 ± 27	< 0.001	0.03	0.02	0.46
Work anaerobic threshold (watts)	29 ± 24	54 ± 18	< 0.001	23 ± 8	52 ± 19	< 0.001	0.94	0.3	0.7
VO _{2max} (mL/min/kg)	14 ± 4 (<i>n</i> = 19)	21 ± 5 (<i>n</i> = 18)	< 0.001	14 ± 4	21 ± 6	< 0.001	0.4	0.5	0.7
VO ₂ anaerobic threshold (mL/kg/min)	11 ± 2	14 ± 4 (<i>n</i> = 18)	0.003	10 ± 3	12 ± 4	0.08	0.5	0.2	0.06
VE/VCO ₂ slope	34 ± 6 (<i>n</i> = 18)	28 ± 5 (<i>n</i> = 19)	0.004	32 ± 5 (<i>n</i> = 17)	28 ± 8	0.09	0.2	0.4	0.2

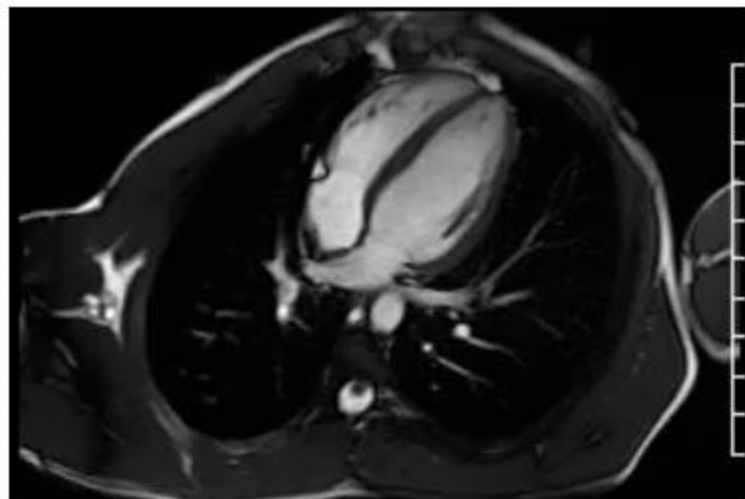
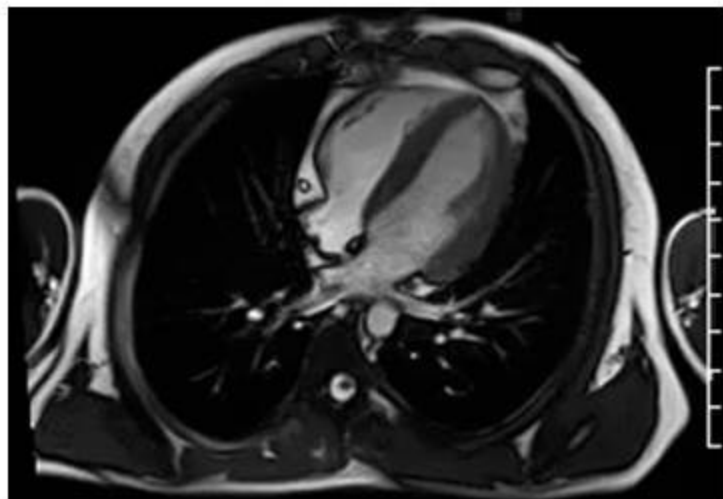
Data are expressed as mean ± standard deviation. FA: Friedreich's ataxia; VE/VCO₂: ventilatory flow/exhaled volume of carbon dioxide; VO₂: oxygen uptake.

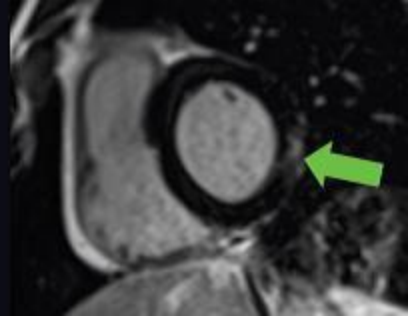
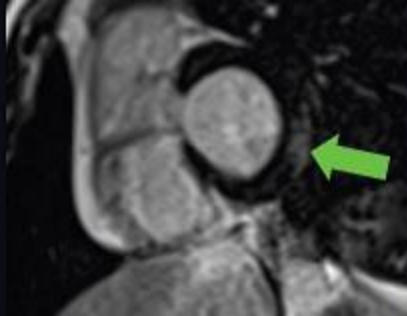
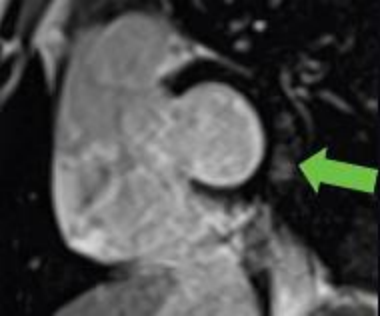
^a *P* compares changes between FA versus control during the study.

^b *P* value compares FA versus control using the Wilcoxon rank sum test.

^c *P* value assesses significance of the change from visit 1 to visit 2 using the Wilcoxon signed rank test.

P compares changes between FA versus control during the study.



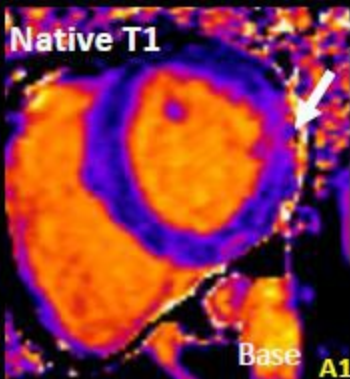


FA Patient

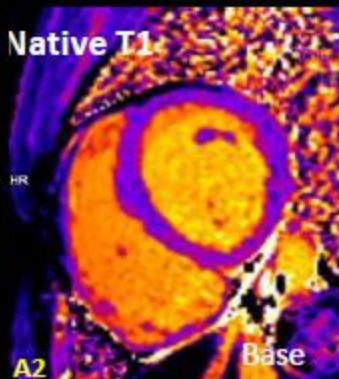
vs

Control

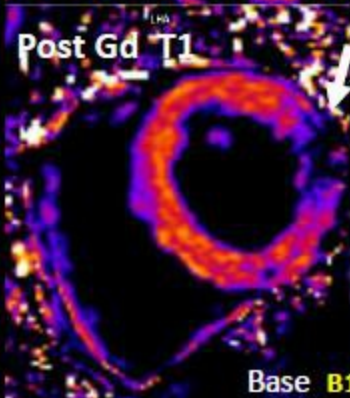
Native T1



Native T1



Post Gd T1



Post Gd T1

